SEA SURFACE WIND RETRIEVAL USING BOTH NORMALIZED RADAR CROSS SECTION AND POLARIZATION RESIDUAL DOPPLER FREQUENCY FROM TERRASAR-X DATA

Faozi Saïd

University of Tromsø
Department of Physics and Technology
N-9037 Tromsø, Norway

Harald Johnsen

Northern Research Institute
Earth Observation Group
N-9294 Tromsø, Norway

ABSTRACT

The polarization residual Doppler frequency (difference between the VV and HH Doppler centroids) is investigated as a valid parameter in a sea surface SAR wind retrieval scheme. This parameter along with the normalized radar cross section are used as inputs to two purely theoretical geophysical model functions based on the Generalized Curvature Ocean Surface Scattering model. A cost function minimization is implemented as part of the proposed wind retrieval method. The methodology is tested using 21 co-polarized TerraSAR-X scenes where retrieved winds are compared against collocated in situ measurements. A 5.23 degree bias along with a 45.3 degree standard deviation and 0.88 correlation are obtained for the wind direction comparison, while a 1.49 m/s bias, 2.36 m/s standard deviation, and 0.72 correlation are obtained for the wind speed comparison.

Index Terms— Doppler measurements, geophysical measurements, radar cross section, sea surface, synthetic aperture radar

1. INTRODUCTION

Sea surface wind retrieval using single look complex SAR data is a challenging task due to the underdetermined nature of the problem [1]. The exclusive use of the normalized radar cross section (NRCS) in such endeavor is insufficient and requires the use of ancillary data. Studies have shown, however, that various geophysical parameters related to the sea surface can be retrieved using the SAR Doppler signal [2] [3] [4]. [5] proposes a method in which the Doppler anomaly (i.e. the difference between the observed and predicted Doppler centroids) is implemented in a sea surface wind retrieval scheme. In this paper, we propose the use of the polarization residual Doppler frequency (PRDF–difference between the observed VV and HH Doppler centroids) combined with the NRCS in a wind retrieval scheme. The wind signature in the Doppler signal is first discussed. Secondly, a wind retrieval methodology incorporating both NRCS and PRDF is described. Finally, results are provided using several co-polarized TerraSAR-X scenes selected in the Norwegian sea.

2. WIND SIGNATURE IN DOPPLER FREQUENCY

The major challenge of using the SAR Doppler signal in wind retrieval applications is the ability to isolate its wind signature. By definition, the Doppler centroid (Dc) is a quantity that is strictly dependent on geometry and instrument related variables as shown in the following equation

$$Dc = \frac{2V_s \sin\theta_{sq,c}}{\lambda}, \tag{1}$$

where V_s is the satellite inertial velocity, $\theta_{sq,c}$ is the squint angle at the beam center crossing time, and λ is the carrier signal's wavelength [6]. Equation 1 holds true over land, but is insufficient to properly describe the Dc over the ocean. Studies have shown that surface currents [3], wave orbital motion and thus the sea surface wind field [2] [7], do affect the Dc over ocean. In order to effectively use the Dc information in a wind retrieval scheme, it is necessary to eliminate the geometric contribution to the Dc as well as reduce the possible mean surface current contribution.

[8] describes the mean surface current contribution to the Dc as zeroth-order Doppler frequencies. Since the geometric and the mean surface current contributions are both polarization independent, the use of co-polarized SAR data can help in reducing these while isolating the wind signature in the Doppler signal. This can be done by computing the polarization residual Doppler frequency (PRDF) as shown in the following equation

$$\Delta Dc = Dc_{VV} - Dc_{HH}, \tag{2}$$

where ΔDc represents the PRDF, while Dc_{VV} and Dc_{HH} the Dc at the VV and HH polarizations, respectively. Estimating the PRDF should completely eliminate the geometric contribution to the Dc and significantly reduce the mean surface current contribution. Using a purely theoretical geophysical Doppler model function (GCM-Dop) based on the Generalized Curvature Ocean Surface Scattering model (GCM) [9] [10], it is possible to simulate the PRDF in terms of wind field. Figure 1 shows the variation of simulated Dc at both polarizations as well as the corresponding PRDF, in terms of wind

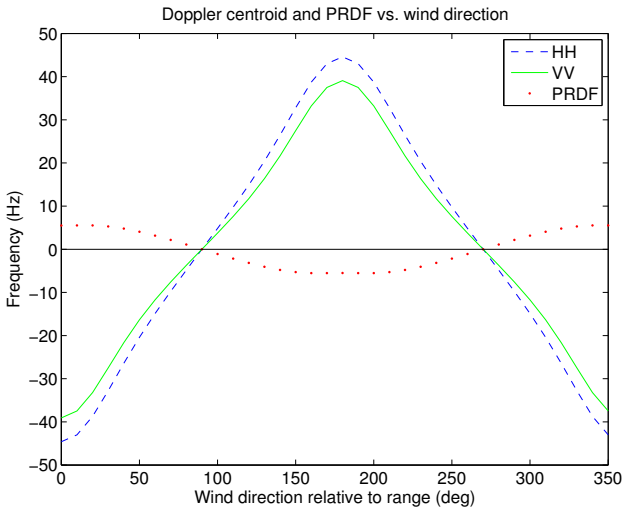

Fig. 1. Plot of the Dc variation at both polarizations, in terms of wind direction relative to range using the GCM-Dop at X-band. The corresponding PRDF (Dc_{VV}-Dc_{HH}) is also plotted. The incidence angle is 25 degrees and the wind speed is 5 m/s. As predicted, the absolute Dcs are zero in crosswind and maximum in up and downwind.

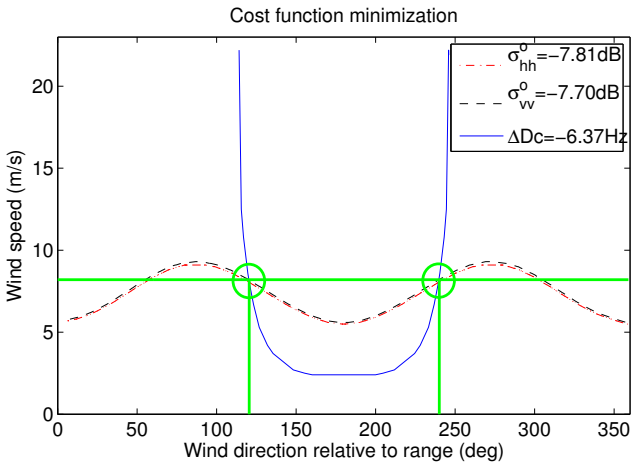

Fig. 2. Plot of a cost function minimization showing the two wind solutions (circled in green) given a measured PRDF of -6.37Hz, a -7.81dB σ^o_{hh}, a -7.70dB σ^o_{vv}, with an assumed 0.84 iwa. Each curve shows the wind speed variation, in terms of the wind direction, for each aforementioned TerraSAR-X measurement. Note that both wind solutions share the same wind speed.

direction relative to range at X-band for a 25 degree incidence angle, a 5 m/s wind speed, and an assumed inverse wave age (iwa) of 0.84. Thanks to a polarization dependency in the sea surface Doppler frequency [7], the PRDF is non-zero for all wind directions except in crosswind conditions (90 and 270 deg) as expected; note that its minimum and maximum are at upwind (180 deg) and downwind (0 deg), respectively.

3. WIND RETRIEVAL METHODOLOGY

Before introducing our wind retrieval scheme which uses both NRCS and PRDF observations, this section first highlights classical wind retrieval methods using radar backscatter signals.

3.1. Classical method

NRCS from scaterrometer or SAR instruments is a variable commonly used in classical sea surface wind retrieval schemes. In order to relate it to actual wind variables, the use of semi-empirical geophysical model functions (GMFs) is required. Such transfer functions have the following general form

$$\sigma^o = B_0[1 + B_1\cos(\phi) + B_2\cos(2\phi)]^z. \quad (3)$$

In this equation, ϕ is the wind direction relative to range, the coefficients B_0, B_1, and B_2 are related to the wind speed, local incidence angle, polarization state, radar frequency , and the exponent z is a tuning parameter [1]. Most GMFs are specifically designed to work at a single polarization state (usually VV), and tuned to optimally perform at a specific radar operating frequency. If needs be, a common method to convert the GMF's σ^o_{vv} to σ^o_{hh} involves the use of a polarization ratio as shown on the right-hand side of the following equation

$$\sigma^o_{hh} = \sigma^o_{vv} \cdot (\frac{\sigma^o_{hh}}{\sigma^o_{vv}})_{MODEL}. \quad (4)$$

This polarization ratio is derived either semi-empirically or analytically [9] [11].

Due to the harmonic nature of equation 3, a single observed σ^o value leads to multiple wind solutions (usually called wind ambiguities). In order to successfully reduce the number of wind ambiguities, the use of ancillary data (e.g. from numerical weather prediction models or in situ data) is necessary, where wind direction is the common requested parameter.

3.2. Wind retrieval using both NRCS and PRDF

As mentioned in the previous section, the GCM-Dop can relate the Dc to the wind field given polarization, incidence angle, radar frequency, and iwa. A second GMF (GCM-NRCS) is likewise derived from the GCM to relate the NRCS to the wind field given the same parameters [9] [10]. Given the incidence angle, polarization, and iwa, the modeled NRCS and PRDF become functions of wind speed and direction only. For a set of observed NRCS and PRDF values, wind solutions can then be retrieved by minimizing the following cost

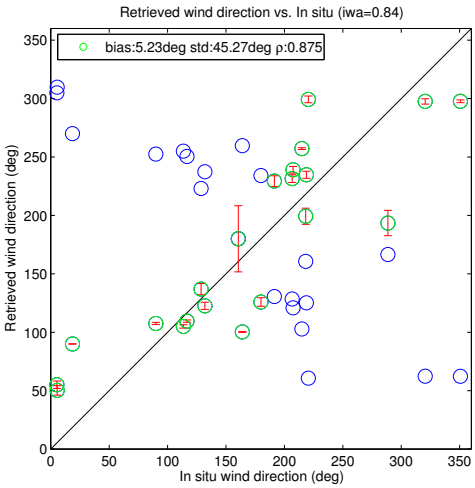

Fig. 3. Scatterplot of retrieved vs. in situ wind directions for an iwa of 0.84. Two wind solutions are plotted against collocated in situ data. The closest of the two is selected and statistics are computed accordingly. Strong correlation is found with a non negligible standard deviation. Error bars are also plotted showing the standard deviation in the selected wind solution due to a +/- 10% variation in iwa.

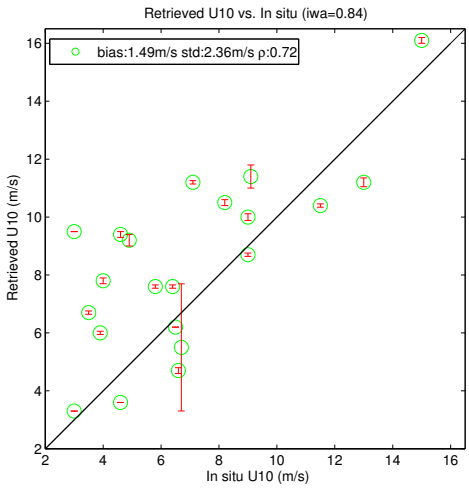

Fig. 4. Scatterplot of retrieved vs. in situ wind speed for 21 TerraSAR-X scenes. Note a slight positive bias yet with fair correlation and standard deviation. Error bars are also plotted showing the standard deviation in wind speed due to a +/- 10% variation in iwa.

function

$$J = \sum_{j=hh}^{vv} \frac{\left(\sigma^o_{jM}(\underline{u}) - \sigma^o_{jOb}\right)^2}{\mathrm{Var}\left(\sigma^o_{jOb}\right)} + \frac{\left(\Delta Dc_M(\underline{u}) - \Delta Dc_{Ob}\right)^2}{\mathrm{Var}\left(\Delta Dc_{Ob}\right)}, \quad (5)$$

where $\mathrm{Var}\left(\sigma^o_{jOb}\right)$ and $\mathrm{Var}\left(\Delta Dc_{Ob}\right)$ represent the variances of the observed NRCS and PRDF values, $\sigma^o_{jM}(\underline{u})$ and $\Delta Dc_M(\underline{u})$ are the predicted NRCS and PRDF from the GCM-NRCS and GCM-Dop, respectively, as a function of the wind field $\underline{u}$, σ^o_{jOb} and ΔDc_{Ob} are the observed NRCS and PRDF over a resolution cell, and the index j represents the polarization state. Figure 2 shows the minimization result using TerraSAR-X data for an incidence angle of 27.1 degrees, a measured PRDF of -6.37Hz, a -7.81dB σ^o_{hh}, a -7.70dB σ^o_{vv}, and an assumed 0.84 iwa. Three curves are shown in this figure describing the wind speed variation in terms of wind direction given the three respective TerraSAR-X measurements (e.g. the solid curve shows how the wind speed varies given the measured PRDF). This plot shows in the given conditions, that the minimization of equation 5 leads to two wind vector solutions, both sharing the same magnitude (i.e. wind speed). As Fig. 2 shows, the two wind direction solutions do not necessarily share a 180 degree ambiguity. In fact, both solutions will either be exclusively up or downwind relative to the radar antenna. Furthermore, depending on the observed PRDF, it is possible to obtain more than two wind vector solutions (i.e. the dotted curve in Fig. 2 crossing the other curves more than twice). In such conditions, minimizing equation 5 may lead to incorrect wind solutions. In any case, it is important to note that these results are obtained without the use of ancillary data, although with an assumed iwa. In the following section, this methodology is implemented with several TerraSAR-X scenes and results are compared with in situ data.

4. WIND RETRIEVAL RESULTS IN X-BAND

21 co-polarized TerraSAR-X scenes (each $\sim$ 17km by 56 km) have been retrieved in the Norwegian sea in proximity to in situ weather stations. Each scene is broken down on a 1x1km grid where both σ^o and Dc are estimated at both polarizations. Note that the σ^o estimation is performed with the addition of an illumination correction based on the local incidence angle as per TerraSAR-X user manual recommendation [12]; the Dc estimation is performed by finding the best fit of a Hanning window to the observed Doppler spectrum. Such technique is used since the Doppler spectrum has a Hanning window applied to it in the SAR processing steps [12].

To simplify the analysis, both σ^o and Dc are then averaged over the whole scene to end up with only one σ^o_{HH}, σ^o_{VV} and ΔDc per scene. These values are then used in the wind retrieval process described in subsection 3.2. For each scene, two wind solutions are recorded and compared with spatially and temporally collocated in situ data (within a 160km radius and 30mn time frame). Figure 3 shows the retrieved wind direction solutions versus in situ wind direction for the 21 TerraSAR-X scenes for an iwa of 0.84. The closest of the

two solutions to in situ wind direction is selected and statistics are computed accordingly. Error bars shown on the selected solutions refer to the standard deviation due to a +/- 10% variation in iwa. The correlation between the selected wind solutions to in situ is strong (0.88) while the standard deviation is substantial (45.3 deg). Figure 4 shows the unambiguously retrieved versus in situ wind speed for the same dataset. There is a slight positive bias of 1.49 m/s compared to in situ with a 2.36 m/s standard deviation. A few solutions do deviate noticeably from in situ results in Fig. 4, particularly in low wind speed situations. After careful analysis, it has been concluded that these outliers are probably due to a filter implementation (Hanning window) in the TerraSAR-X Multimode SAR Processor; such filter use can adversely modify the original spectrum and negatively impact the Doppler centroid estimation [4]. It has also been found that a very small change in the observed Doppler centroid value can greatly affect the wind retrieval results. Nevertheless, overall results are very satisfying and show the potential of using the observed PRDF combined with corresponding observed NRCS in SAR wind retrieval processes.

5. CONCLUSION

In this paper, an alternate sea surface SAR wind retrieval approach is presented where both observed NRCS and PRDF are used along with two GCM based GMFs. A cost function minimization is used to find the appropriate wind solutions for 21 co-polarized TerraSAR-X scenes. Comparison is made against in situ data. Correlation coefficients for both wind direction and speed retrievals are high, though with non negligible biases and standard deviations. This is to show that the PRDF can certainly be used in a sea surface wind retrieval scheme, and help drastically reduce the number of wind ambiguities without the use of ancillary data. The presented approach does require however the use of co-polarized SAR data combined with geophysical model functions relating both NRCS and Doppler signal to wind variables, and the assumption of an iwa.

Future work may include a separate wind direction estimation process from the SAR data itself, to help further reduce the wind ambiguity solutions. In addition, the GCM based GMFs rely on a sea surface description where the skewness factor can be improved.

6. REFERENCES

[1] Marcos Portabella Arnús, *Wind Field Retrieval from Satellite Radar Systems*, Astronomy and meteorology department, University of Barcelona, September 2002.

[2] Bertrand Chapron, Fabrice Collard, and Fabrice Ardhuin, "Direct measurements of ocean surface velocity from space: interpretation and validation," *Journal of Geophysical Research*, vol. 110, no. C07008, 2005, doi:10.1029/2004JC002809.

[3] Fabrice Collard, Alexis A. Mouche, Bertrand Chapron, Céline Danilo, and Johnny Johannessen, "Routine high resolution observation of selected major surface currents from space," in *Proceedings of SEASAR 2008, SP-656*, ESA - ESRIN, Frascati, Italy, 2008, ESA.

[4] C. Rossi, H. Runge, H. Breit, and T. Fritz, "Surface current retrieval from terrasar-x data using doppler measurements," in *Geoscience and Remote Sensing Symposium (IGARSS), 2010 IEEE International*, july 2010, pp. 3055 –3058.

[5] K-F. Dagestad, A. Mouche, F. Collard, M.W. Hansen, and J. Johannessen, "On the use of doppler shift for sar wind retrieval," in *SeaSAR Workshop 2010, ESA-ESRIN*, Italy, January 2010.

[6] Ian G. Cumming and Frank H. Wong, *digital processing of SYNTHETIC APERTURE RADAR DATA*, chapter Doppler Centroid Estimation, ARTECH HOUSE, 2005.

[7] Ida Friestad Pedersen, Geir Engen, and Harald Johnsen, "Polarization dependency in sea surface doppler frequency and its application to envisat asar alt-pol data," in *Envisat and ERS Symposium*. Norut Information Technology, September 2004.

[8] Roland Romeiser and Donald R. Thompson, "Numerical study on the along-track interferometric radar imaging mechanism of oceanic surface currents," *IEEE Transactions on Geoscience and Remote Sensing*, vol. 38, no. 1, pp. 446–458, 2000.

[9] Geir Engen, Ida Friestad-Pedersen, Harald Johnsen, and Tanos Elfouhaily, "Curvature effects in ocean surface scattering," *IEEE Transactions on Antennas and Propagation*, vol. 54, no. 5, pp. 1370–1379, May 2006.

[10] Harald Johnsen, Geir Engen, and Gilles Guitton, "Sea-surface polarization ratio from envisat asar ap data," *IEEE Transactions on Geoscience and Remote Sensing*, vol. 46, no. 11, pp. 3637–3646, November 2008.

[11] A. Mouche, D. Hauser, J.-F. Daloze, and C. Guérin, "Dual polarization measurements at C-band over the ocean: Results from airborne radar observations and comparison with ENVISAT ASAR data," *IEEE Transactions on Geoscience and Remote Sensing*, vol. 43, pp. 753–769, 2005.

[12] M. Eineder, T. Fritz, J. Mittermayer, A. Roth, E. Borner, and H. Breit, *TerraSAR-X Ground Segment Basic Product Specification Document*, German Aerospace Center (DLR), Germany, October 2010.